16th World Conference on Earthquake Engineering, 16WCEE 2017
Santiago Chile, January 9th to 13th 2017
Paper N° 1641
Registration Code: S-Y1464687622

EXPERIMENTS ON CRESCENT SHAPED BRACE, A NEW SIMPLE HYSTERETIC BRACING DEVICE

A. Dib [1], M. Palermo [2], S. Silvestri [3], T. Trombetti [4]

[1] *PhD Student, University of Bologna, antoine.dib2@unibo.it*
[2] *Researcher, University of Bologna, Michele.palermo7@unibo.it*
[3] *Professor, University of Bologna, Stefano.silvestri@unibo.it*
[4] *Professor, University of Bologna, tomaso.trombetti@unibo.it*

Abstract

Over the last fifty years, extensive researches have been conducted in the field of seismic isolation systems, innovative earthquake resisting systems and supplemental damping, showing a potential step towards the boosting of the seismic performance of buildings.

The Crescent Shaped Braces (CSB) is a new simple steel hysteretic device, recently proposed by some of the authors to be used as an enhanced diagonal brace in framed structures, within the Performance Based Design framework. By making use of CSBs as lateral resisting system, thanks to the peculiar shape of such devices, the seismic design may be optimized due to the uncoupling of its lateral stiffness from its yield strength.

In the present study, the main results of experimental tests conducted on scaled CSB specimens (designed according to simplified design formulas developed by the authors) realized with different cross-sections are presented. Both monotonic pseudo-static tests and cyclic tests have been performed in order to further assess the seismic behavior of such devices. The overall experimental response in terms of stiffness, strength, ductility and global instability is compared with the design formulations, while the detailed hysteretic response is compared with the results of numerical simulations developed with commercial software. It is shown that the overall experimental behavior of CSBs is well captured by the design formulas and that commercial software are suitable to simulate the hysteretic response of such device.

Keywords: Crescent shaped Braces, New hysteretic Devices, Performance Based Seismic Design, Dissipative Devices.

1. Introduction

Within the framework of the Performance Based Seismic Design (PBSD), the current seismic design tendencies have a goal to go beyond the traditional earthquake-resistance philosophy (that accepts damages as long as life safety is guaranteed) and minimize damage to structural and nonstructural elements, avoid failures, loss of life and keep construction costs reasonable. These design approaches use supplemental damping and/or seismic isolation systems, so that the building structure should behave in the desired way under frequent, occasional, rare and very rare seismic events. Furthermore, the main elements of the structure are protected by diverting the seismic energy to these mechanical devices that can be inspected and even replaced following an earthquake. As a result, one of the design strategies beneath the PBSD is the conceptual separation of the vertical resisting system from the horizontal one, which allows the achievement of multiple performance objectives. Theoretically, the main structure will be intact from any damage in the case that the seismic energy induced by the earthquake on the building is absorbed totally by the dampers [1].

Many studies have been carried out on special typologies of steel bracing elements (hysteretic devices, friction devices, eccentric bracing systems…). In particular, metallic and friction (hysteretic) dampers belong to the category of displacement-activated supplemental damping systems. They take advantage of displacement of the hysteretic behavior of metals when deformed into the post-elastic range to dissipate energy [1, 3]. The most relevant developments in this line are the following devices: The Added Damping – Added Stiffness (ADAS) device, originally manufactured by Bechtel Corporation in the 1980s, is usually installed between the apex of a chevron brace and the underside of the beam. The Triangular Added Damping – Added Stiffness (TADAS) device, is a variation of the original ADAS device which makes use of triangular plates as dissipative steel elements [2]. The Buckling Restrained Brace (BRB) consists in a steel member encased in a tube filled with concrete that prevents the buckling [4]. The Cast Steel Yielding Fuse (CSF) device, as the one manufactured by Cast Connex Corporation (under the name of Scorpion Yielding Devices), is a steel devices for concentrically braced frames which dissipates energy through inelastic flexural yielding of special elements [5] and the Crescent Shaped Braces (CSB) developed by the University of Bologna, is a hysteretic device presented in this paper.

The Crescent Shaped Brace (CSB) device was first introduced by some of the authors as an enhanced diagonal brace able to fulfill multiple seismic design objectives in terms of stiffness, strength and ductility [6]. Then, CSB devices has been used to realize an enhanced first-storey isolated building with high seismic performances, inspired by the original concept of storey isolation proposed in the late 1960s by Fintel and Khan [7], with superior seismic performances.

The CSB device, thanks to its boomerang geometrical shape, is characterized by a lateral stiffness uncoupled from the yield strength and, in certain cases, by a symmetric hysteretic behavior with a fast increase in the stiffness at large lateral drifts which may prevent from global structural instability due to second-order effects (P-Δ Effects).

In a previous work [8], analytical and numerical studies devoted to the assessment of the non-linear mechanical and geometrical behavior of CSB have been presented, with a particular attention devoted to design purposes. In the present study, the results of different experimental tests conducted on scaled CSB specimens of different cross-section under both monotonic and reversed pseudo-static cyclic loads are presented in order to assess their experimental cyclic behavior.

2. The seismic behavior of Crescent Shaped Braces

2.1 The geometry

The Crescent Shaped Brace (CSB) is a lateral hysteretic resisting steel device composed of two straight members which are connected with a specific angle. Its peculiar shape can be “ad hoc” defined in order to assess an independently desired behavior in terms of both lateral stiffness and yielding strength, on the contrary of common bracing devices, where these two parameters are dependent [6, 9].

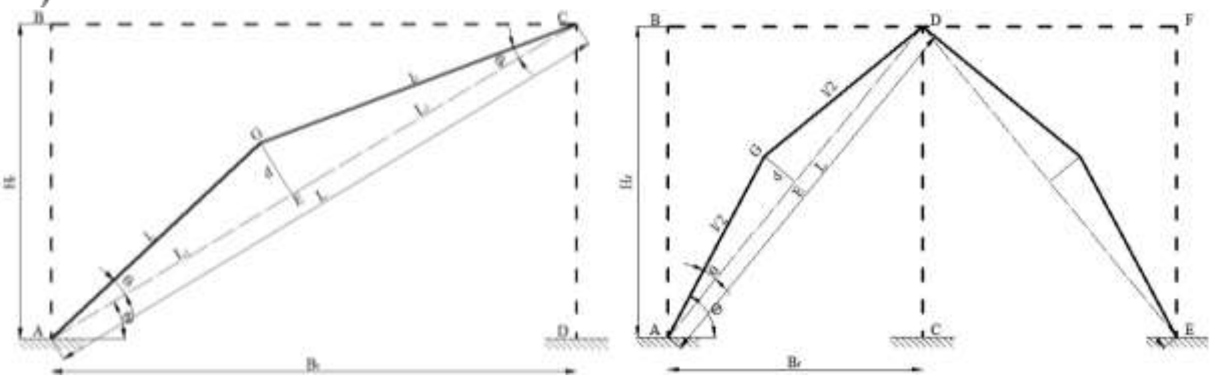

Fig. 1 – Geometry of CSBs inserted in a frame: (Left) bilinear configuration; (Right) doubly symmetrical configuration

The CSB devices can be inserted in a frame either in a bilinear configuration or in a doubly symmetrical configuration as shown in Fig.1.The geometrical characterizations of the frame are the following: B_f is the frame width. H_f is the frame height. L is the length of the diagonal of the frame or the projection of the CSB. Θ is the inclination of the reference diagonal. θ is the inclination of the elements of the CSB in reference to the diagonal. l1 and l2 are respectively the length of the two elements of the device (in the study presented here, l1= l2= l). d, referred to as "arm", is the orthogonal distance between the knee point G and the reference point E on the diagonal line.

2.2 The response of CSBs under lateral loads

In a previous works [6, 8, 9] the behaviour of a CSB device subjected to lateral loads has been fully described with both analytical and numerical studies. In detail, simple analytical formulas have been proposed to predict the strength under tension and compression.

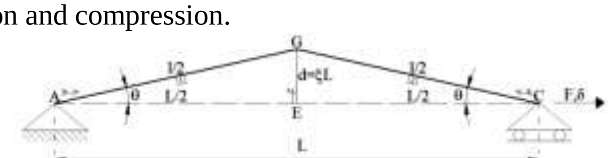

Fig. 2 – The geometrical configuration of the studied CSB

From a strength-design perspective, the behaviour of a CSB under a positive F, Fig. 2, (i.e. a lateral force inducing a tension axial force in each member) can be described in terms of:

- The lateral force leading to the first yielded point at the knee section, F_{pl}:

$$N_d = \frac{M_{pl}}{d} \tag{1}$$

- The maximum tensile capacity of the CSB is reached for a lateral load F leading to the complete elongation of the CSB, i.e. when the lever arm d and the angle θ drop to zero. The axial plastic capacity N_{pl} of the straight member:

$$N_{pl} = A \cdot f_y \tag{2}$$

When the device is subjected to negative F (inducing compression in each member), the element is expected to act elastically until it reaches the yield point and then it experience a softening response due to non-linear geometrical effects. The equations governing the response are:

$$\begin{aligned} F_e &= K_L \cdot \delta && \text{for } \delta \le \delta_y \\ F_{pl} &= M_{pl}\left(d_0 + \delta/2 \tan \Delta\theta\right) && \text{for } \delta > \delta_y \end{aligned} \tag{3}$$

Where F_d and F_{pl} indicates the response within the elastic and plastic fields, respectively:

$$K_L = 3EJ\Delta\theta \Big/ \left(2 \cdot l^2 \cdot \sin^2\theta . \left(\cos\theta_0 - \cos\theta\right)\right) \tag{4}$$

K_L is the approximate lateral (flexural) stiffness of the system (neglecting second-order effects). The initial lateral stiffness is equal to

$$K_{L0} = 3EJ / (l^3 \cdot \sin^2(\theta_0)) \tag{5}$$

The rotation θ is related to the lateral and vertical displacements v and δ through the following trigonometric relationships:

$$\begin{aligned} \delta &= 2 \cdot \left(\cos\theta_0 - \cos\theta\right) \cdot l \\ v &= \left(\sin\theta - \sin\theta_0\right) \cdot l \end{aligned} \tag{6}$$

The value of the yielding displacement can be rigorously obtained by solving the following transcendent non-linear equation:

$$K_L \cdot \delta_y = \frac{M_{pl}}{\left(d + \delta_y / \tan\theta_y\right)} \tag{7}$$

Nonetheless, the force and the displacement leading to the formation of the plastic hinge can be approximately evaluated by imposing the equilibrium in the initial un-deformed configuration (first order approximation):

$$\begin{cases} F_{pl0} = M_{pl} / d_0 \\ \delta_{y0} = F_{pl0} / K_{L0} \end{cases} \tag{8}$$

3. Experimental Tests

3.1 The experimental campaign to assess the behaviour of CSBs devices

To evaluate the cyclic pseudo-static response of CSB devices, four experimental campaigns have been scheduled at the laboratories of the University of Bologna, Italy, between 2014 and 2016. Results of the first two campaigns were presented in a previous work [9]. A summary of all the results of the four campaigns is presented in the following parts.

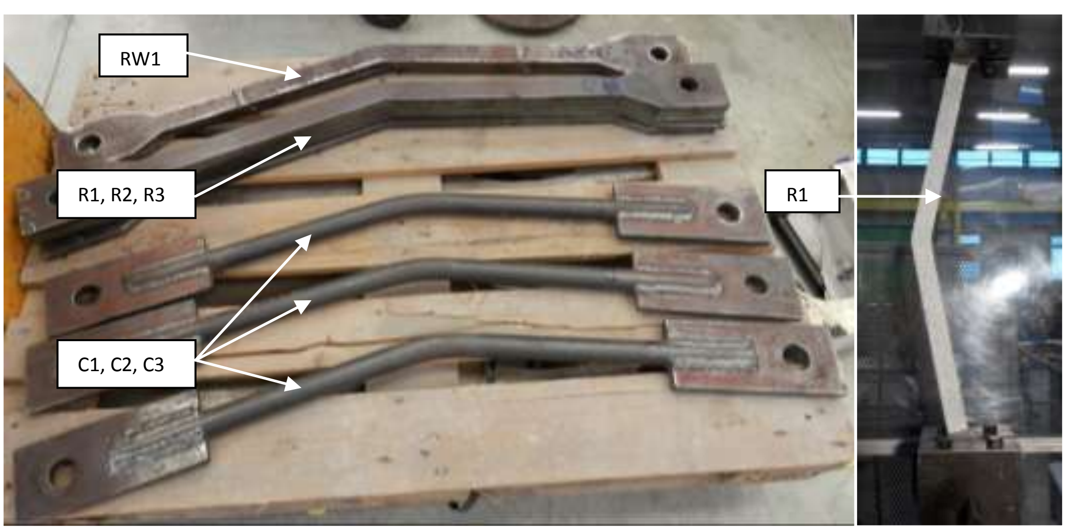

Fig. 3 – The CSB specimens: left) before the test, right) under test

3.2 The tested specimens and the test protocols

In the first campaign, three rectangular specimens, R1, R2 and R3with a cross section of 1.5 cm x 4.14 cm were tested. The second test was dedicated to test three fully circular specimens, C1, C2, C3 with a circular cross section of diameter "D" equal to 35 mm. While welded CSB with rectangular cross section RW1 and rectangular cross section CSB with welded ribs RR1 were tested in the third campaign, the fourth one was devoted to test tubular circular welded cross section TW1. All The specimens are 1/6 scaled, therefore representative of a brace inserted in a rectangular frame of 3 m (height) x 6 m (span).

The tests were carried out using a universal tensile machine Metro Com with a nominal capacity of up to 600 kN. The machine allows adjusting the test conditions varying both the load, through the pressure of the fluid and the speed, through a flow regulator. The instrumentation is supplemented by a system of acquisition and processing of data [8].

All CSB specimens are made of S275JR steel (according to EN 10025) with average measured yielding stress of 330 MPa and the ultimate tensile stress ranged between 470 and 490 MPa.

Table 1 – The main geometrical characteristics of the tested specimens and the load protocol

Specimen	Loading Protocol	h [mm]	*A* [mm^2]	*J* [mm^4]	*L* [mm]	ξ [-]
R1-T	Tensile	41.4	621	8870	1040	0.10
R2-C	Compression	41.4	621	8870	1040	0.10
R3-R	Reversed	41.4	621	8870	1040	0.10
RR1-R	Reversed	41.4	770	8920	1040	0.10
RW1-C+T	Compression + Tensile	41.4	621	8870	1040	0.10
C1-T	Tensile	35.0	962	8990	980	0.10
C2-C	Compression	35.0	962	8990	980	0.10
C3-R	Reversed	35.0	962	8990	980	0.10
TW1-R	Reversed	42.0	333	6470	1060	0.10

As mentioned in table 1, the specimen with the letter T were subjected to tensile loads, the ones with the letter C were subjected to compression loads while the ones with letter R were subjected to reversed cyclic loads.

The test protocols, corresponding to tensile, compression and reversed loadings are displayed in Fig. 4.

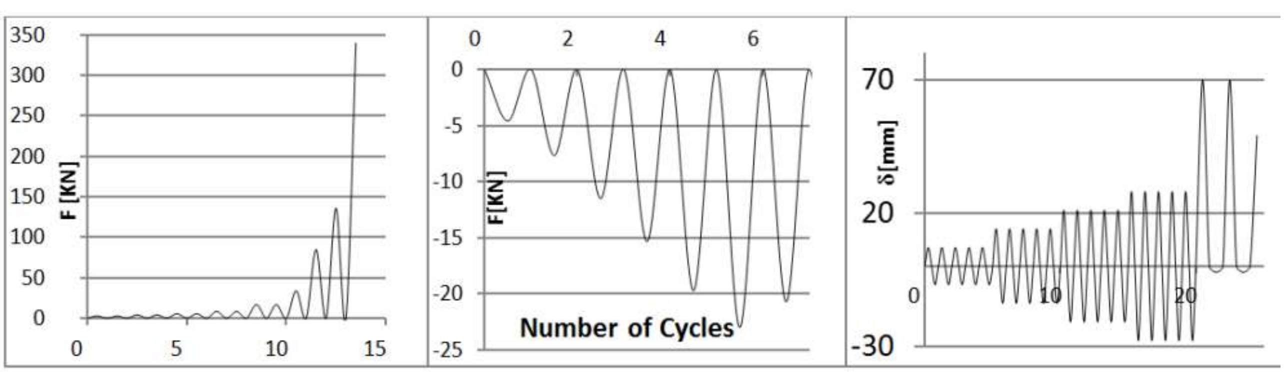

Fig. 4 –left) Tensile test protocol, middle) Compression test protocol, right) Reversed test protocol

4. The Experimental force-displacement response

4.1 The force-displacement responses

The experimental force-displacement responses for all the tested specimens are shown in Fig. 5. The recorded responses include the small displacements due to the slacks related to the oversized holes. The two rectangular R1-T and R2-C specimens and the two circular C1-T and C2-C specimens exhibited a stable in-plane cyclic behavior under tensile and compressive loads. On the contrary, the rectangular R3-R specimen buckled out-of-plane when subjected to cyclic compression after yielding in tension due to the unfavorable height-to-width ratio (around 3) leading to a reduced out-of-plane moment of inertia. The circular C3-R specimen did not buckle out-of-plane. Similarly, the rectangular RR1-R, thanks to the presence of the ribs leading to a significant increase in the out-of-plane moment of inertia, did not show a significant out-of-plane response. The rectangular welded RW1-C+T showed a stable cyclic in-plane behavior under the initial cycles in compression and also during the subsequent cycles in tension up to the end of the test. The tubular welded TW1-R showed a not stable cyclic behavior with a progressive degradation of the tensile strength.

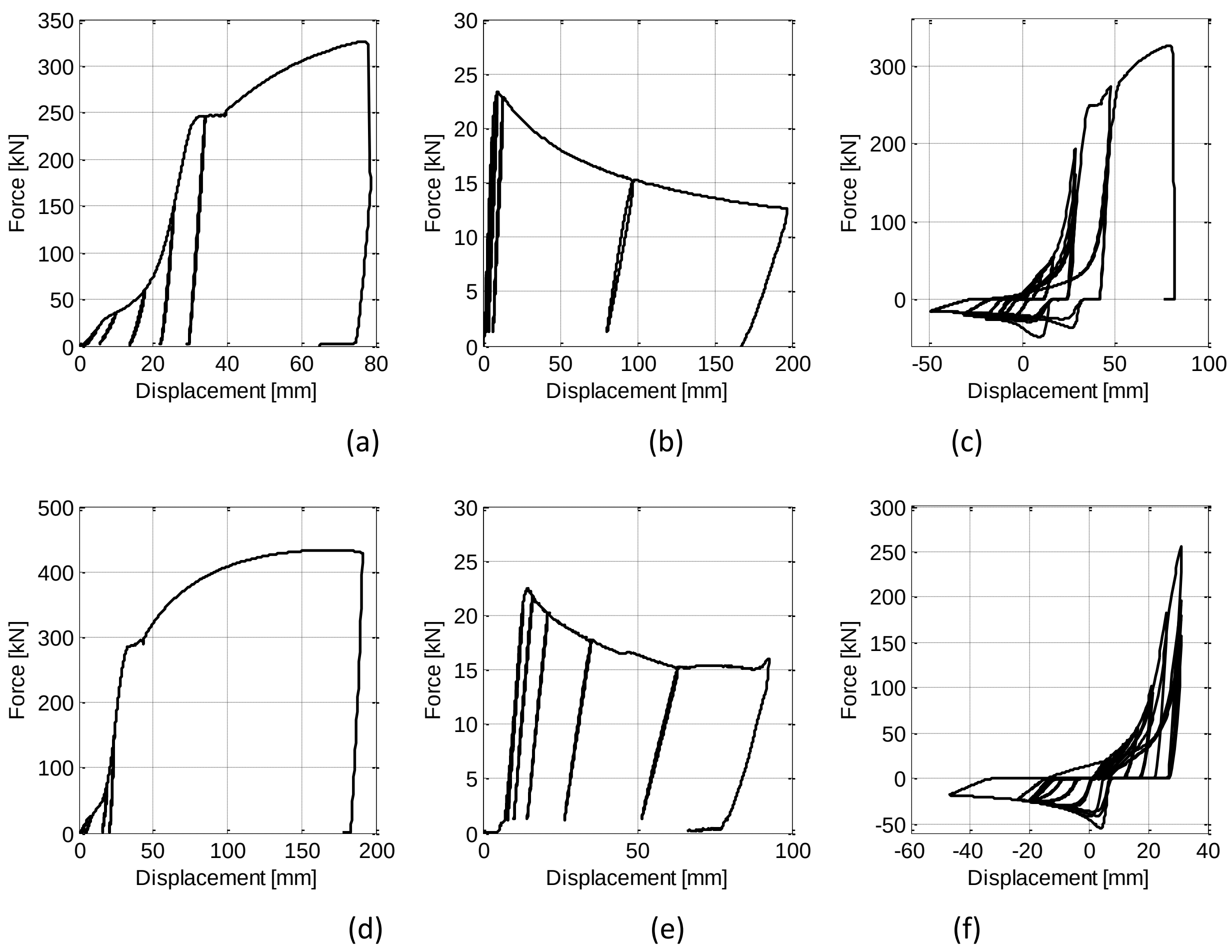

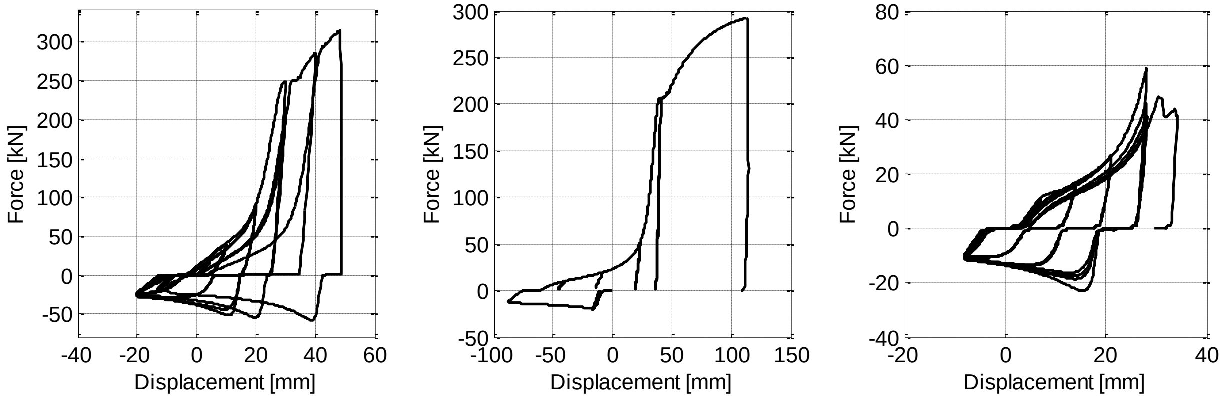

(g) (h) (i)

Fig. 5–Experimental force-displacement cyclic response for specimen (a) R1-T; (b) R2-C; (c) R3-R; (d) C1-T; (e) C2-C; (f) C3-R; (g); RR1-R; (h) RW1-C+T (i) TW1-R;

4.2 Initial lateral stiffness, first yielding force and maximum lateral force

The values of the initial lateral stiffness K_{L0}, the lateral forces leading to the first yielding F_y and the maximum recorded forces F_{max} obtained from the experimental tests are reported in Table 2 and compared with the predictions as given by Eqs. 1, 2, 5and 8.The values of the experimental force leading to the first yielding F_y are obtained from visual inspection of the recorded force-displacement response.

Table 2 – Initial lateral stiffness, first yielding force and maximum lateral force.

	K_{L0} [kN/mm]		F_y [kN]		$F_{\max}$ [kN]		
Specimen	Experimental	Eq.5	Experimental	Eq.1	Experimental	Eq.8	Eq.2
R1-T	4.2	4.8	17	15.5	324	23.2	248
R2-C	4.0	4.8	16	15.5	22	23.2	248
R3-R	3.4(C) ÷ 4(T)	4.8	10(C) ÷ 15(T)	15.5	22(C) ÷ 320(T)	23.2	248
RR1-R	4.1(C) ÷ 6(T)	4.9	15(C) ÷ 20(T)	15.7	57(C) ÷ 300(T)	23.6	308
RW1-C+T	3.6 (C)	4.8	15 (C)	15.5	18(C) ÷ 290(T)	23.2	248
C1-T	3.9	4.7	18	16.3	420	27.7	385
C2-C	3	4.7	15	16.3	21.3	27.7	385
C3-R	3.3(C) ÷4.7(T)	4.7	10(C) ÷ 11(T)	16.3	54(C) ÷ 250*(T)	27.7	385
TW1-R	2.7(C) ÷2.7(T)	3.4	6(C) ÷ 8(T)	10.7	22(C) ÷ 58(T)	14.4	133

(*) the test was stopped at the first signs of ovalization of the holes

4.3 Experimental Envelopes vs 1-DOF analytical responses and numerical responses

The envelope of experimental force-displacement response as obtained from the cyclic tests in tension and compression on the full rectangular and full circular specimen (i.e. R1-T, R2-C and C1-T, C2-C) are shown in Fig. 6 (thick –black line) and compared with the numerical response (thin-black line) and the analytical response (red line) of the 1-DOF mechanical system as described before. In the numerical simulation the steel material is characterized by: an elastic modulus E= 200000 MPa, a yield stress fy based on the results of material tensile tests, a hardening ratio r=0.5%. In tension, up to a lateral displacement of 15 mm, both the analytical response of the 1-DOF mechanical system and the numerical response are practically coincident with the experimental envelopes. Then, for larger displacement under tensile loadings the analytical 1-DOF response becomes very stiff given that the axial flexibility has been neglected; the numerical response is still slightly stiffer than the experimental envelopes. In compression, both the analytical 1-DOF response and the numerical response are able to accurately capture the experimental envelopes.

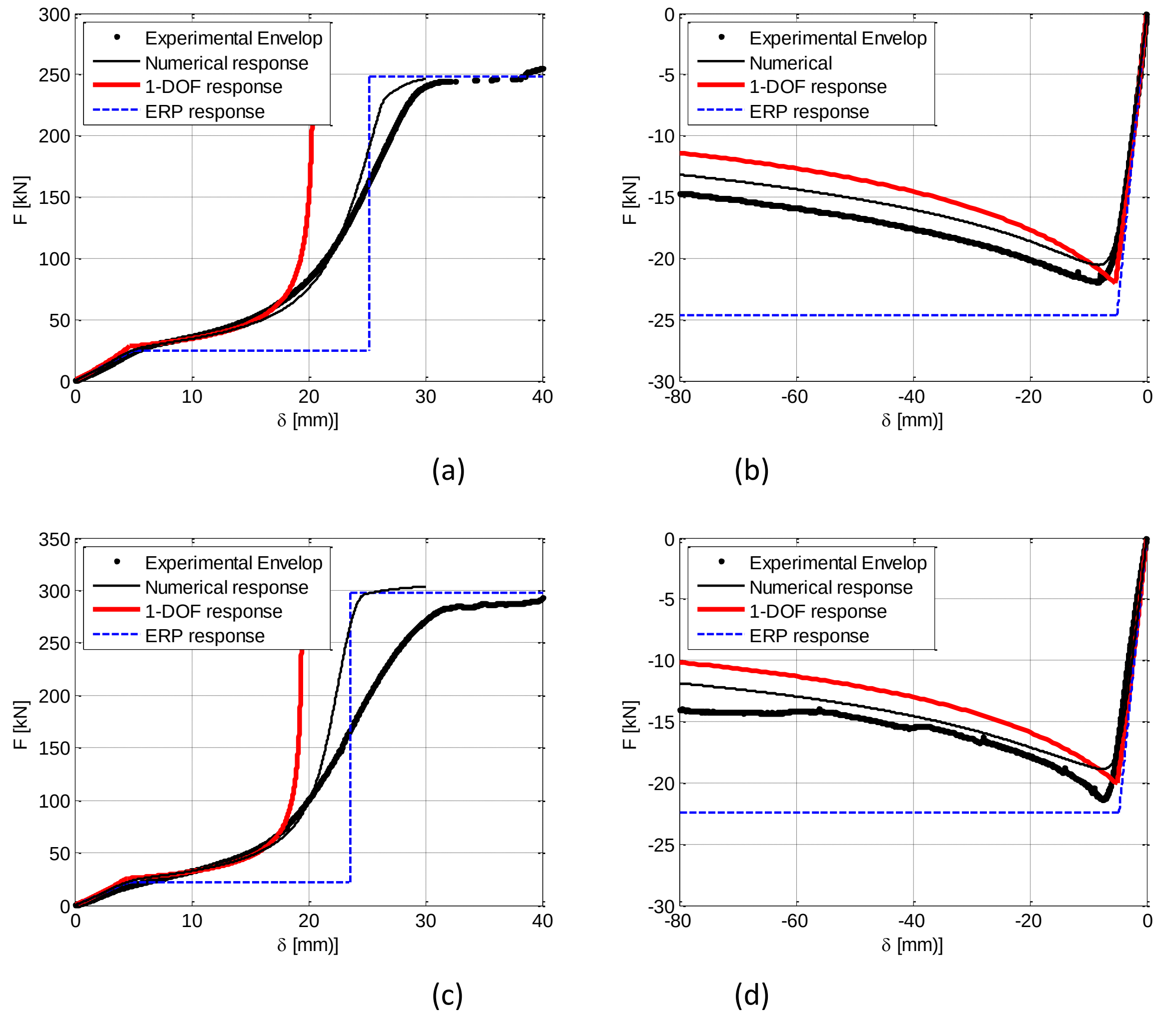

Figure 6– Experimental envelop vs analytical and numerical response: (a) R1-T; (b) R2-C; (c) C1-T; (d) C2-C.

4.4 Deformation fields

The Digital Image Correlation (DIC) technique is used to monitor the surface deformation field. The monitoring is performed using a VIC-3D HR system, with a hardware composed by two cameras with a resolution of 14 Megapixel (in terms of deformation the resolution is around 50 me). In order to adopt the DIC camera, the surface of the specimen is treated with white painting and black dots.

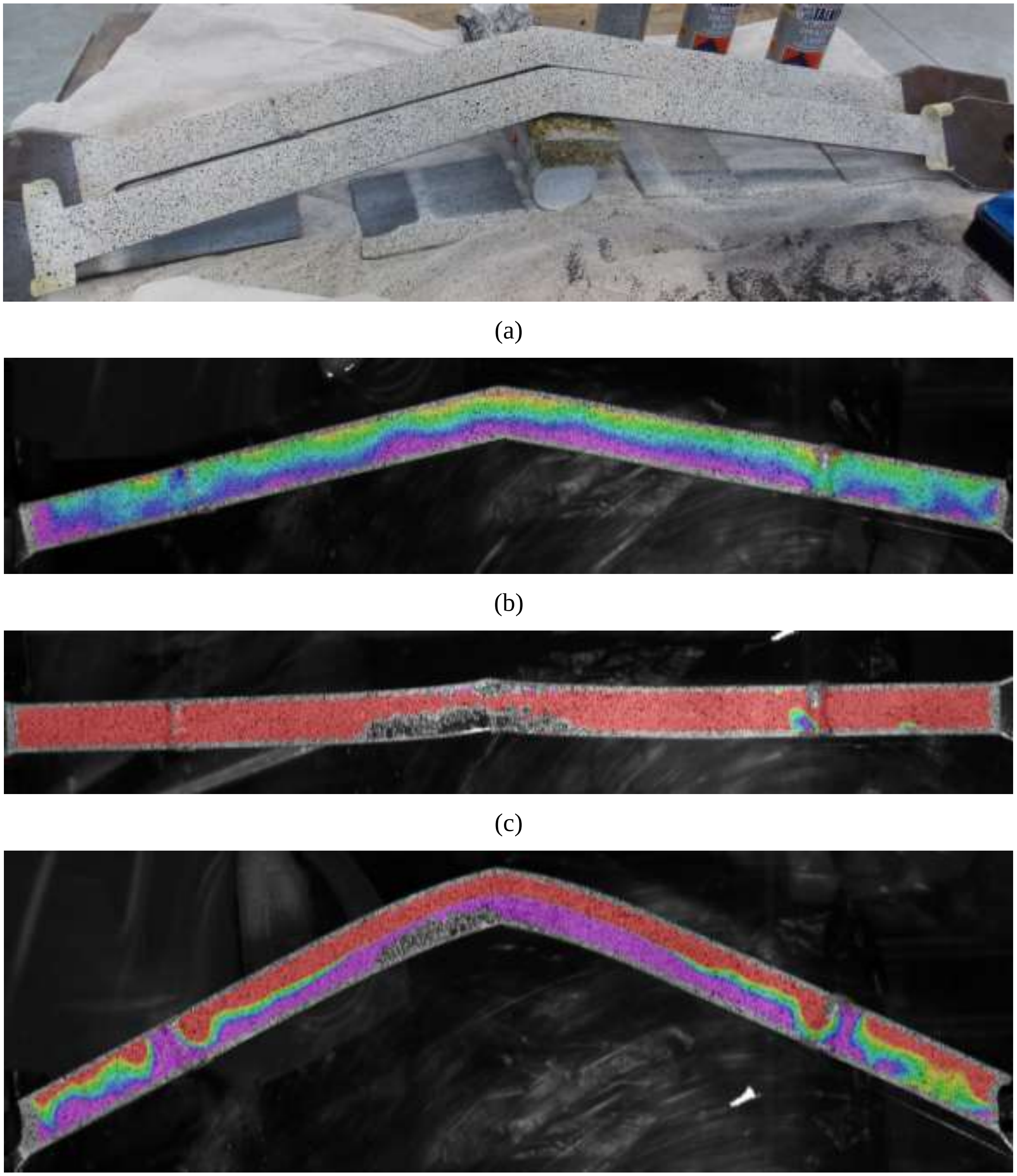

(a)

(b)

(c)

(d)

Figure 7– Specimens' stresses verified by the DIC: a) specimens R3 and RW1 before the test, b) specimen RW1, c) specimen R1 after yielding, d) specimen RW1 under compression load

For the specimen RW1, tested under cyclic tensile and compression test, when it reaches the maximum displacement, the maximum stresses (Red color) are verified near the knee zone and not the welded part. Regarding compression test, it is clear from the DIC technique, that the concentration of the stresses (violet color) is spread in the knee zone and around it.

(a)

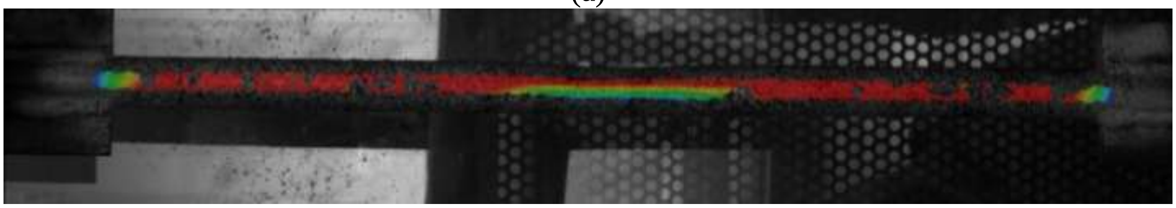

(b)

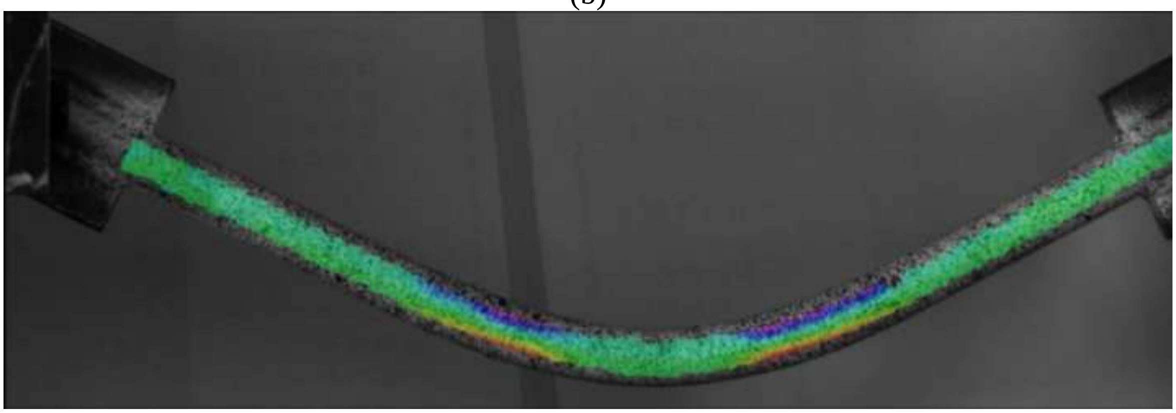

(c)

Figure 8– specimens' stresses verified by the DIC: a) a specimen before the test, b) specimen C1, c) specimen C2

For the specimen C1, tested under cyclic tensile test, when it reaches the maximum displacement, the maximum stresses (Red color) are verified near the knee zone. Regarding the specimen C2, which was tested under cyclic compression test, it is clear from the DIC technique, that the concentration of the stresses (violet color) is spread, not in the knee zone (green color), but around it.

This phenomenon can be related to the fact that the knee was bent, thus, this zone knew a hardening and resists more both under tensile and compression loads.

5. Conclusion

In the present paper, a new hysteretic device, the crescent shaped braces (CSB), is presented. In details, the results of four experimental campaigns devoted to assess the nonlinear cyclic behavior of rectangular section, full circular section, ribbed welded rectangular section and tubular circular section have been presented.

From design point of view, the device, due to its boomerang geometrical shape, has a number of desirable seismic properties, such as the initial lateral stiffness uncoupled from the first yield strength, a significant ductile capacity and a final hardening which prevents from P-Δ effects.

Simplified analytical models are presented in order to capture the main features of the experimental response, i.e. the stiffness, yield strength and inelastic response and verified the experimental results, thus suggesting that CSBs could be efficiently used as an enhanced alternative to the conventional steel diagonal concentric brace or the more advanced buckling resisting braces and scorpion devices.

The results of the experimental campaign showed that rectangular profiles with a large height-to-width ratio tend to experience significant out-of-plane buckling after exposed to large elongations in tension. Such effect is prevented by using cross sections with larger out-of-plane moment of inertia, such as the circular and the rectangular with ribs cross sections.

CSB made by two straight members welded at the knee cross section experienced a sudden premature fragile failure at the knee section. Thus, when it is not possible to obtain a device from a unique element (laser-cut manufactured), the welding should be realized far from the knee sections and from the ends of the members.
On overall, the experimental findings confirm the expected theoretical behavior of the device, thus suggesting that CSBs could be efficiently used as an enhanced alternative to the conventional steel diagonal concentric brace or the more advanced buckling resisting braces and scorpion devices.
To complete the experimental assessment, the next experimental tests will be carried out on a specific CSBs disposition which is characterized by a theoretically symmetric hysteretic response and by a superior dissipation capacity.

6. References

[1] Christopoulos, C., Filiatrault, A., & Bertero, V. V. (2006). Principles of passive supplemental damping and seismic isolation. Iuss press

[2] Tsai, K. C., Chen, H. W., Hong, C. P., & Su, Y. F. (1993). Design of steel triangular plate energy absorbers for seismic-resistant construction. Earthquake spectra, 9(3), 505-528.

[3] Robinson, W., & Greenbank, L. (1976). An extrusion energy absorber suitable for the protection of structures during an earthquake. Earthquake Engineering & Structural Dynamics, 4(3), 251-259.

[4] Gleim S., Dorka U. E., (2008), A design method for hysteretic Device Systems, 14 WCEE, Beijing, China.

[5] Gray, M. G., Christopoulos, C., & Packer, J. A. (2010, July). Cast steel yielding fuse for concentrically braced frames. In Proceedings of the 9th US National and 10th Canadian Conference on Earthquake Engineering (Vol. 9). Oakland, CA, USA and Ottawa, ON, Canada: Earthquake Engineering Research Institute and the Canadian Association for Earthquake Engineering.

[6] Trombetti, T., Silvestri, S., Gasparini, G., & Ricci, I. (2009). Stiffness-Strength-Ductility-Design Approaches for Crescent Shaped Braces. Open Construction and Building Technology Journal, 3, 127-140.

[7] Fintel, M., & Khan, F. R. (1968). Shock-Absorbing Soft Story Concept for Multistory Earthquake Structures. Portland Cement

[8] Palermo, M., Silvestri, S., Gasparini, G., & Trombetti, T. (2015). Crescent shaped braces for the seismic design of building structures. Materials and Structures, 48(5), 1485-1502.

[9] Dib A, Palermo M, Pieraccini L, Silvestri S, Gasparini G, Trombetti T (2015) Experiments on Crescent Shaped Braces, ISEC -08